

## Synthesis, Optical Properties and Thermal Stability of Octa(*p*-chlorophenoxy) Substituted Phthalocyanine Complexes of Magnesium(II) and Zinc(II)

Elena A. Gorbunova, Yana N. Korovkina, Alina S. Agranat,  
Tatyana B. Shatalova, and Tatiana V. Dubinina<sup>@</sup>

Department of Chemistry, Lomonosov Moscow State University, 119991 Moscow, Russian Federation  
<sup>@</sup>Corresponding author E-mail: dubinina.t.vid@gmail.com

*The present study is a continuation of the work on the synthesis and study of the properties of octa(*p*-chlorophenoxy)-substituted phthalocyanines. In the previous study, the optical characteristics of the lutetium complex were described. The present work is devoted to zinc and magnesium complexes. Comparative studies of absorption and luminescence spectra were carried out. The thermal stability of the target compounds up to 800 °C was studied by thermogravimetry with synchronous mass spectrometric analysis.*

**Keywords:** Phthalocyanines, template synthesis, spectroscopy, fluorescence, thermal stability.

## Синтез, оптические свойства и термическая стабильность окта(*пара*-хлорфеноксизамещенных фталоцианиновых комплексов магния(II) и цинка(II)

Е. А. Горбунова, Я. Н. Коровкина, А. С. Агранат, Т. Б. Шаталова, Т. В. Дубинина<sup>@</sup>

Химический факультет, Московский государственный университет имени М.В. Ломоносова, 119991 Москва, Российская Федерация  
<sup>@</sup>E-mail: dubinina.t.vid@gmail.com

*Настоящее исследование является продолжением работы по синтезу и изучению свойств окта(*пара*-хлорфеноксизамещенных фталоцианинов. В предыдущем исследовании были описаны оптические характеристики комплекса лютеция. Настоящая работа посвящена комплексам цинка и магния. Проведены сравнительные исследования спектров поглощения и люминесценции. Термическая устойчивость целевых соединений вплоть до 800 °C исследована методом термогравиметрии с синхронным масс-спектрометрическим анализом.*

**Ключевые слова:** Фталоцианины, темплатный синтез, спектроскопия, флуоресценция, термическая стабильность.

### Introduction

Phthalocyanines are macrocyclic compounds that are structurally related to natural porphyrins. The main advantages of phthalocyanines in comparison with porphyrins are high extinction coefficients of absorption ( $\lg \epsilon \geq 5$ ) at the

border of the visible and near IR regions and photochemical stability.<sup>[1,2]</sup>

Due to their unique photophysical and photochemical properties, phthalocyanines and their metal complexes are widely used as optical limiters,<sup>[3,4]</sup> sensors,<sup>[5]</sup> and components of photovoltaic cells.<sup>[6-8]</sup> In addition, phthalocyanines

are currently being investigated as promising photosensitizers for the photodynamic therapy (PDT) of cancer and photodynamic antimicrobial chemotherapy (PACT).<sup>[9,10]</sup>

The introduction of functional groups along the periphery of the macrocycle improves the solubility of the complexes, as well as bathochromically shifts the absorption maximum to the region of high transparency of biological tissues (600–900 nm).<sup>[11]</sup> The introduction of electron-withdrawing groups, such as halogens, helps to increase oxidation resistance due to the anodic shift of the first oxidation potential.<sup>[12,13]</sup> At the same time, the attachment of halogen atoms directly to the macrocycle results in low solubility of phthalocyanines in organic solvents.<sup>[14]</sup> The presence of a flexible phenoxy spacer between the halogen atom and the phthalocyanine macrocycle leads to a decrease in  $\pi$ - $\pi$  interactions and aggregation. Thus, the presence of halogen-phenoxy substituents in phthalocyanines improves their solubility compared to halogen-substituted analogs.

The present study is a continuation of our work on the synthesis and study of the properties of octa(*p*-chlorophenoxy)-substituted phthalocyanines.<sup>[15]</sup> In the previous study, the optical characteristics of the lutetium(III) complex were described. The present work is devoted to complexes with zinc and magnesium, which were chosen as central ions to study the relationship between structure and optical properties.

Magnesium phthalocyanine complexes, like zinc complexes, are capable of generating singlet oxygen, and for this reason they can be used in the treatment of cancer or bacterial infections. However, compared with zinc complexes, the yields of singlet oxygen generation for these compounds are much lower. Magnesium phthalocyanines are mainly used as bright fluorophores.<sup>[16,17]</sup>

## Experimental

All reactions were monitored by thin-layer chromatography (TLC) and UV-Vis spectroscopy until complete disappearance of the initial compounds unless otherwise specified. TLC was performed using Merck Aluminium Oxide F<sub>254</sub> neutral flexible plates. The electronic absorption spectra (UV-Vis) were recorded on a JASCO V-770 spectrophotometer using quartz cells (1×1 cm). Matrix assisted laser desorption/ionization time-of-flight (MALDI TOF) mass spectra were registered on Bruker Autoflex II mass spectrometer without matrix. The salts Zn(OAc)<sub>2</sub>×2H<sub>2</sub>O and Mg(OAc)<sub>2</sub>×4H<sub>2</sub>O were dried at 60 °C for 3 h immediately before use. Attenuated Total Reflection–Fourier Transform Infrared spectroscopy (ATR-FTIR) was carried out using Thermo Scientific Nicolet iS5 FT-IR spectrometer. Spectral resolution:  $\Delta\lambda = 4 \text{ cm}^{-1}$ . <sup>1</sup>H NMR spectra were recorded on a Bruker AVANCE 600 (600.13 MHz) spectrometer. Chemical shifts are given in ppm relative to SiMe<sub>4</sub>. Fluorescence spectra were recorded on «Fluorite -02-Panorama» spectrophotometer using quartz cells with an optical path length of 1 cm at room temperature. Fluorescence quantum yields of phthalocyanines were recorded in DMF using zinc phthalocyanine as a reference compound ( $\Phi_f = 0.23$  in THF<sup>[18]</sup>) irradiated with the xenon lamp at 610 nm. The quantum yields of fluorescence were determined by the method described in literature<sup>[19]</sup> according to the formula:

$$\Phi_f^i = \frac{F^i f_s n_i^2}{F^s f_i n_s^2} \Phi_f^s$$

where  $\Phi_f^s$  is the fluorescence quantum yield for the standard,  $F^i$  and  $F^s$  are the areas under the luminescence spectra of the sample and the standard,  $n_i^2$  and  $n_s^2$  are the squares of the refractive indices in the used solvent for the sample and standard, respectively.  $f_i = 1 - 10^{-A_x}$ , where  $A_x$  is the absorption of the sample at the registration wavelength.

Thermal behavior was investigated by TG-DTA analysis using NETZSCH STA 449 F3 Jupiter combined with mass-spectrometry analysis of TGA gas phase products using NETZSCH QMS 403 Aëolos Quadro, Germany. Measurements were performed in alund crucibles at a heating rate of 10 K/min under oxygen atmosphere (50 mL/min).

**4,5-(*p*-Chlorophenoxy)phthalonitrile (1).** A mixture of 4,5-dichlorophthalonitrile (1.00 g, 5.1 mmol) and *p*-chlorophenol (3.84 g, 30 mmol) was dissolved with DMF (15 mL) and placed in a flask. The reaction was carried out at 90 °C in an argon atmosphere. Anhydrous K<sub>2</sub>CO<sub>3</sub> (17.00 g, 123 mmol) was added in portions every 5 min. Then the reaction mass was stirred for 30 min. Formed precipitate was filtered off and recrystallized from MeOH to give compound **1** (1.37 g, 71%) in the form of a cream-colored powder. MS (MALDI-TOF) *m/z*: 381 [M], 317 [M-2Cl], 253 [M-Cl(*p*-ClPhO)]. MS (MALDI-TOF/TOF) *m/z*: 381.0120 [M]. Calculated for C<sub>20</sub>H<sub>10</sub>Cl<sub>2</sub>N<sub>2</sub>O<sub>2</sub>: 381.0192 [M]. <sup>1</sup>H NMR (400 MHz, CDCl<sub>3</sub>)  $\delta_{\text{H}}$  ppm: 7.00 (d, 4H, H<sub>1</sub>), 7.20 (s, 2H, H<sub>Ar</sub>), 7.40 (d, 4H, H<sub>2</sub>). <sup>13</sup>C NMR (100 MHz, CDCl<sub>3</sub>)  $\delta_{\text{C}}$  ppm: 152.56, 151.39, 131.27, 130.60, 122.35, 120.95, 114.65 (CN), 110.99 (C-CN).

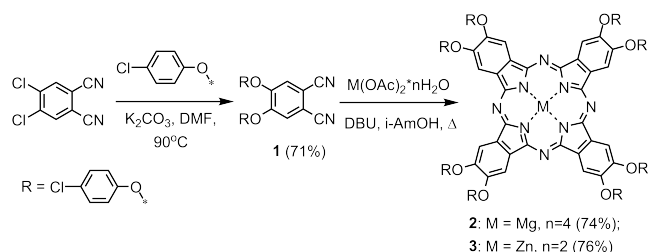
**Magnesium 2,3,9,10,16,17,23,24-octa(*p*-chlorophenoxy)-phthalocyaninate (2).** A mixture of phthalonitrile (150.0 mg, 0.4 mmol), Mg(OAc)<sub>2</sub>×4H<sub>2</sub>O (21.5 mg, 0.25 mmol) and DBU (14.9  $\mu$ L, 0.1 mmol) was refluxed in isoamyl alcohol (1.5 mL) with stirring for 3 h. The reaction was monitored by TLC (SiO<sub>2</sub>, F<sub>254</sub>, toluene) and UV-Vis spectroscopy (THF). The reaction mixture was cooled to room temperature and MeOH:H<sub>2</sub>O (4:1 V/V) was added. The precipitate was filtered off and washed with MeOH:H<sub>2</sub>O (4:1, V/V) and dried at room temperature. This yielded 114.0 mg (74%) of complex **2**. UV-Vis (THF)  $\lambda_{\text{max}}$  nm (lg $\epsilon$ ): 358 (4.71), 608 (4.32), 675 (5.10). IR (diamond)  $\nu \text{ cm}^{-1}$ : 1024-1079 (st C-Cl); 1079-1335 (st C-O<sub>phenolic</sub>); 1397-1585 ( $\gamma$  heteroaromatic); 3035-3055 (st CH<sub>Ar</sub>). MS (MALDI-TOF) *m/z*: 1451 [M-(*p*-ClC<sub>6</sub>H<sub>4</sub>)+H<sub>2</sub>O]<sup>+</sup>, 1544 [M]<sup>+</sup>. MS (MALDI TOF/TOF) *m/z*: 1544.0327 [M]<sup>+</sup>; Calculated for C<sub>80</sub>H<sub>40</sub>Cl<sub>8</sub>N<sub>8</sub>O<sub>8</sub>Mg: 1544.0328 [M]<sup>+</sup>. <sup>1</sup>H NMR (600.13 MHz, THF-*d*<sub>8</sub>)  $\delta_{\text{H}}$  ppm: 7.17 (d, 16H, *J* = 8.3 Hz, H<sub>1</sub>), 7.39 (d, 16H, *J* = 8.3 Hz, H<sub>2</sub>), 9.10 (s, 8H, H<sub>Pc</sub>).

**Zinc 2,3,9,10,16,17,23,24-octa(*p*-chlorophenoxy)phthalocyaninate (3).** A mixture of phthalonitrile (150.0 mg, 0.4 mmol), Zn(OAc)<sub>2</sub>×2H<sub>2</sub>O (21.9 mg, 0.25 mmol) and DBU (14.9  $\mu$ L, 0.1 mmol) was refluxed in isoamyl alcohol (1.5 mL) with stirring for 3 h. The reaction was monitored by TLC (SiO<sub>2</sub>, F<sub>254</sub>, toluene). The reaction mass was cooled to room temperature and MeOH:H<sub>2</sub>O (4:1 V/V) was added. The precipitate was filtered off and washed with MeOH:H<sub>2</sub>O (4:1, V/V) and dried at room temperature. This yielded 120 mg (76%) of complex **3**. UV-Vis (THF)  $\lambda_{\text{max}}$  nm (lg $\epsilon$ ): 360 (4.84), 609 (4.45), 675 (5.20). IR (diamond)  $\nu \text{ cm}^{-1}$ : 1027-1088 (st C-Cl); 1087-1265 (st C-O<sub>phenolic</sub>); 1398-1585 ( $\gamma$  heteroaromatic); 3035-3060 (st CH<sub>Ar</sub>). MS (MALDI-TOF) *m/z*: 1492 [M-(*p*-ClC<sub>6</sub>H<sub>4</sub>)+H<sub>2</sub>O]<sup>+</sup>, 1582 [M]<sup>+</sup>. MS (MALDI-TOF/TOF) *m/z*: 1582.9698 [M]<sup>+</sup>; Calculated for C<sub>80</sub>H<sub>40</sub>Cl<sub>8</sub>N<sub>8</sub>O<sub>8</sub>Zn: 1582.9769 [M]<sup>+</sup>. <sup>1</sup>H NMR (600.13 MHz, THF-*d*<sub>8</sub>)  $\delta_{\text{H}}$  ppm: 7.26 (d, 16H, *J* = 8.8 Hz, H<sub>1</sub>), 7.40 (d, 16H, *J* = 8.8 Hz, H<sub>2</sub>), 8.79 (s, 8H, H<sub>Pc</sub>).

## Results and Discussion

To obtain halogen-containing phthalocyanines with high solubility in organic solvents, *p*-chlorophenoxy substituents were introduced at the stage of obtaining the initial nitrile **1** (Scheme 1). Nitrile **1** was prepared through

nucleophilic substitution reaction from 4,5-dichlorophthalonitrile. The optimum temperature and solvent were previously selected using *p*-bromophenoxy substituted phthalonitrile as an example.<sup>[20]</sup> This reaction is activated by the presence of two strong electron-withdrawing CN groups and gives nitrile **1** in good yield. Phthalocyanine complexes **2** and **3** were then prepared by one-step template synthesis (Scheme 1).



**Scheme 1.**

Target complexes were obtained in boiling isoamyl alcohol in the presence of 1,8-diazabicyclo[5.4.0]undec-7-ene (DBU) as a base. Due to the possibility of nucleophilic substitution typical for the electron-deficient systems, the use of DBU as a base is preferred rather than employment of alkali metal alcoholates.<sup>[15]</sup>

The identification of target compounds was performed using high-resolution matrix-assisted laser desorption/ionization time-of-flight (MALDI-TOF) mass spectrometry, <sup>1</sup>H NMR and infrared spectroscopy. The stability of the complexes was investigated, and the presence of chlorine atoms in peripheral positions was confirmed through thermogravimetric study and the results of evolved gas analysis by mass spectrometry.

Mass spectra demonstrated intense peaks of the molecular ions  $[\text{M}]^+$ . In addition, peaks were observed in the mass spectra of the target compounds, which can be attributed to the cleavage of the *p*-ClC<sub>6</sub>H<sub>4</sub> group and the formation of an adduct with water  $[\text{M}-(p\text{-ClC}_6\text{H}_4) + \text{H}_2\text{O}]^+$  (Figure 1). The formation of adducts with water is probably a result of the use of Zn(OAc)<sub>2</sub>·2H<sub>2</sub>O and Mg(OAc)<sub>2</sub>·4H<sub>2</sub>O crystal hydrates with coordinated water in the inner coordination sphere as a source of template ions.

The high resolution mass spectra of complexes demonstrated good agreement between the observed and calculated masses. The experimentally observed isotope patterns for peaks of molecular ions  $[\text{M}]^+$  are in good agreement with theoretically calculated ones.

In order to comprehensively confirm the structure of the target phthalocyanine complexes of zinc and magnesium, as well as to confirm the absence of impurities of the initial phthalonitrile, IR spectra were recorded. Attenuated Total Reflection-Fourier Transform Infra-Red (ATR-FTIR) spectra were measured for thin film on the surface of diamond. Figure 2 shows the IR spectrum of compound **2** as an example.

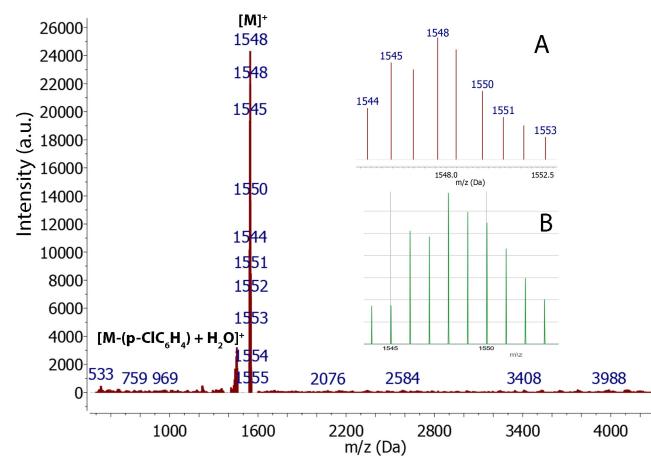
Skeletal vibrations of heteroaromatic fragments ( $\gamma$  heteroaromatic) occupy the region 1397–1585 cm<sup>-1</sup>. The bands at 1024–1079 cm<sup>-1</sup> were assigned to stretching vibrations of C-Cl bonds. Stretching vibrations of C-O of phenolic moieties were observed at 1079–1335 cm<sup>-1</sup>.

Stretching vibrations of aromatic CH fragments were found in the region 3035–3055 cm<sup>-1</sup> (Figure 2). Stretching vibrations of aliphatic CH were observed at 2828 cm<sup>-1</sup>. They can be assigned to residual methanol from the stage of purification of the target complexes.

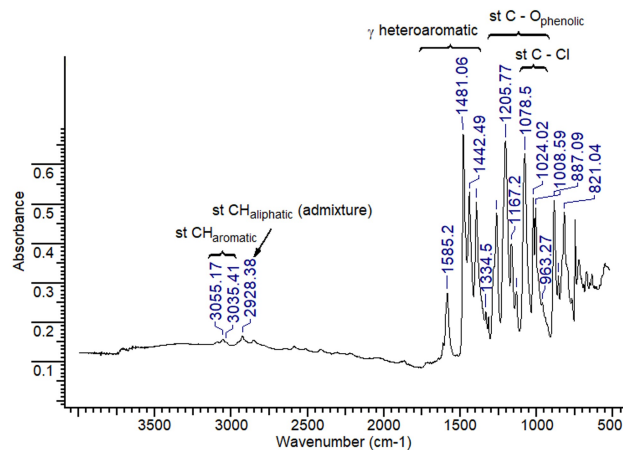
To suppress the aggregation at high concentrations and obtain well-resolved <sup>1</sup>H NMR spectra of target phthalocyanines, the polar coordinating solvent THF-*d*<sub>8</sub> was chosen. The use of pyridine or *N,N*-dimethylformamide (DMF) can help suppress aggregation, but results in overlap of proton signals from the solvent and the sample.

Figure 3 shows the <sup>1</sup>H NMR spectrum of the zinc phthalocyanine complex. Three groups of signals of unequal protons are detected. Two doublets of aromatic protons of aryloxy groups demonstrate a *J*-coupling constant of about ~8 Hz (Figure 3, insets).

UV-Vis spectra of target complexes demonstrated *B* band at 360 nm and intense *Q* band at 675 nm. In this case, the nature of the central metal does not affect the position of the *Q* band (Figure 4).



**Figure 1.** LDI TOF mass spectrum of magnesium complex **2** (without matrix, positive ion mode). The inserts show the experimentally obtained (A) and theoretically calculated (B) isotopic pattern for molecular ion  $[\text{M}]^+$ .



**Figure 2.** ATR-FTIR spectrum of the complex **2** (*p*-ClC<sub>6</sub>H<sub>4</sub>O)<sub>8</sub>PcMg.

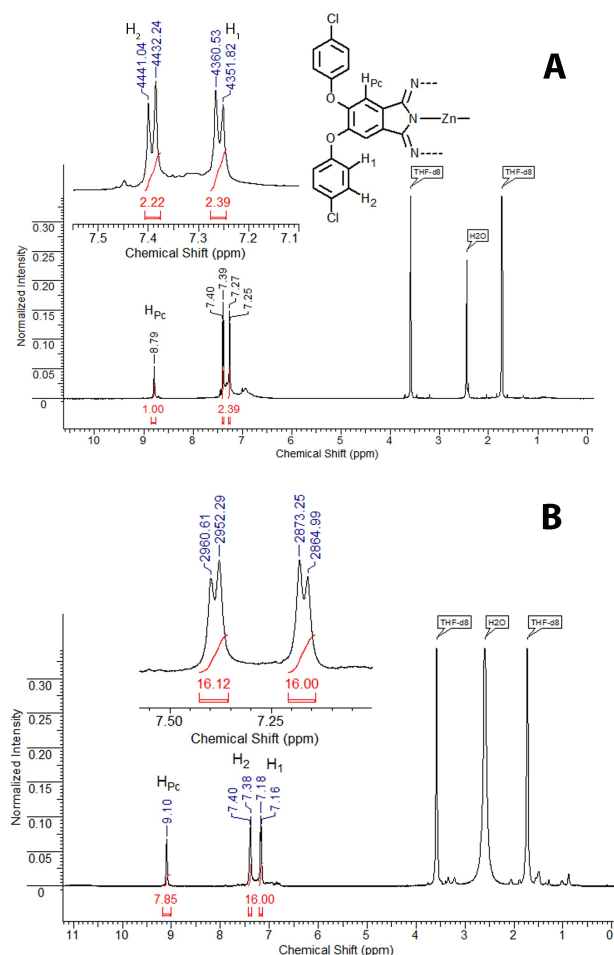


**Figure 3.**  $^1\text{H}$  NMR spectra of zinc **3** (A) and magnesium **2** (B) complexes in  $\text{THF-}d_8$ .

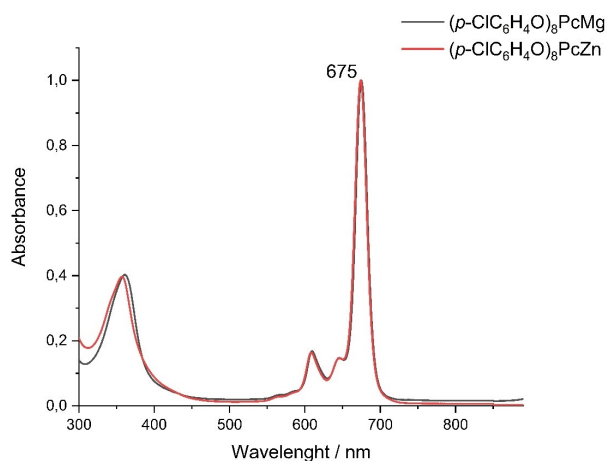


**Figure 4.** UV-Vis spectra of compounds  $(p\text{-ClC}_6\text{H}_4\text{O})_8\text{PcMg}$  **2** and  $(p\text{-ClC}_6\text{H}_4\text{O})_8\text{PcZn}$  **3** measured in THF.

It was shown that the introduction of a phenoxy fragment between the chlorine atom and the periphery of phthalocyanine does not lead to a shift of the Q band relative to octachloro-substituted analogs.<sup>[14]</sup> The introduction of various functional groups into the *para*-position of the aryloxy fragment also does not significantly change the position of absorption maximum compared to phenoxy

substituted phthalocyanines (Table 1). It is important to note that the presence of bulky aryloxy substituents contributes to an increase in solubility in organic solvents compared to chloro-substituted analogues. The extinction coefficients for hexadecachloro-substituted  $\text{Cl}_{16}\text{PcTbOAc}$  are  $\lg\epsilon = 4.43$ ,<sup>[21]</sup> and for complex **2**  $\lg\epsilon = 5.20$ , indicating that the  $\pi\text{-}\pi$  stacking is slightly suppressed and aggregation is correspondingly reduced, leading to improved solubility. The  $\lg\epsilon$  values is 5.10 for  $(p\text{-ClC}_6\text{H}_4\text{O})_8\text{PcZn}$  complex. It was found that the dependence of absorbance on concentration obeys the Beer's law up to  $C=1.5\cdot 10^{-5}$  M for complex **2** and  $2\cdot 10^{-5}$  M for complex **3** (Figure 5).

Emission and excitation spectra were measured for target complexes (Figure 6).

The absorption and excitation spectra of fluorescence coincide, while the excitation and emission spectra are mirror images of each other. For the emission spectrum, a bathochromic shift is observed relative to the absorption spectrum (Stokes shift), since, according to Stokes rule, the frequency of the emitted light is always less than the frequency of the absorbed light. The Stokes shift of the Q bands is 10 nm which is typical for phthalocyanines and their analogs.<sup>[25]</sup> The wavelength of fluorescence emission for all complexes was 677 nm.

The fluorescence quantum yields of phthalocyanines were measured in THF using unsubstituted zinc phthalocyanine as the standard ( $\Phi_f = 0.23$  in THF<sup>[18]</sup>) (Table 2).

**Table 1.** UV-Vis data in different solvents.

| Compound   | Q band, nm | Solvent         | Reference    |
|--|------------|-----------------|--------------|
| <b>2</b>   | 675        | THF             | present work |
| <b>3</b>   | 675        | THF             | present work |
| $(p\text{-ClC}_6\text{H}_4\text{O})_8\text{PcLuOAc}$       | 675        | THF             | [15]         |
|  | 681        | $\text{CHCl}_3$ |              |
| $\text{Cl}_8\text{PcLuOAc}$                                | 676        | THF             | [14]         |
| $(p\text{-MeC}_6\text{H}_4\text{O})_8\text{PcMg}$          | 678        | $\text{CHCl}_3$ | [22]         |
| $(p\text{-MeC}_6\text{H}_4\text{O})_8\text{PcZn}$          | 678        | $\text{CHCl}_3$ |              |
| $(\text{C}_6\text{H}_5\text{O})_8\text{PcZn}$              | 674        | THF             | [18]         |
| $(\text{C}_6\text{H}_5\text{O})_8\text{PcMg}$              | 683        | $\text{CHCl}_3$ | [23]         |
|  | 678        | DMF             |              |
| $(p\text{-}^i\text{BuC}_6\text{H}_4\text{O})_8\text{PcZn}$ | 683        | $\text{CHCl}_3$ | [24]         |
| $(p\text{-NO}_2\text{C}_6\text{H}_4\text{O})_8\text{PcZn}$ | 678        | DMSO            |              |

**Table 2.** Fluorescence data for phthalocyanines in THF.

| Compound                    | Central metal | $\lambda_{\text{em}}$ , nm | $\Phi_f$          | Reference    |
|-----------------------------|---------------|----------------------------|-------------------|--------------|
| <b>2</b>                    | Mg            | 685                        | 0.42              | present work |
| <b>3</b>                    | Zn            | 686                        | 0.21              | present work |
| $(\text{PhO})_8\text{PcZn}$ | Zn            | 686                        | 0.31              | 18           |
| $\text{PcZn}$               | Zn            | 672                        | 0.23              | 18           |
| $\text{PcMg}$               | Mg            | 681 <sup>a</sup>           | 0.23 <sup>a</sup> | 26           |

<sup>a</sup> – spectrum was measured in DMF

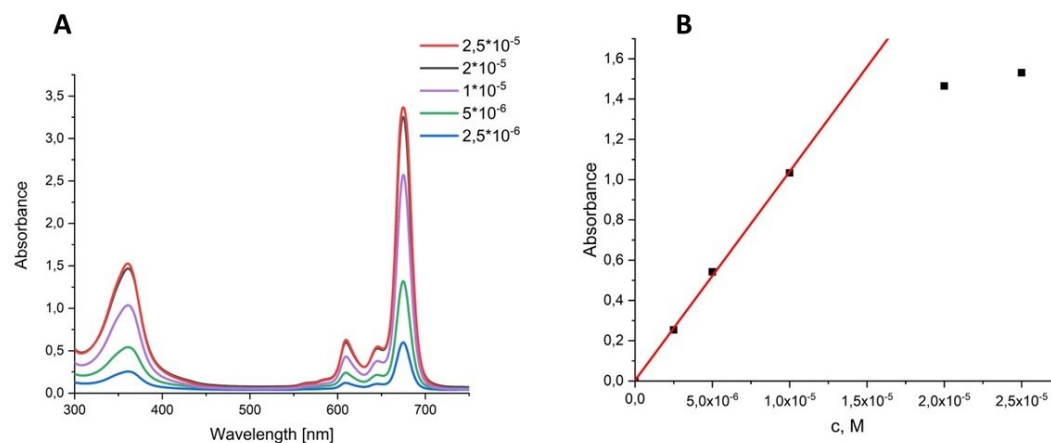


**Figure 5.** UV-Vis spectra of complex **2** diluted from  $C=2.5 \cdot 10^{-5}$  M to  $C=2.5 \cdot 10^{-6}$  M in THF (A). The dependence of the absorption intensity at the maximum of the *Q* band on the concentration, the red line shows the calibration curve (B).

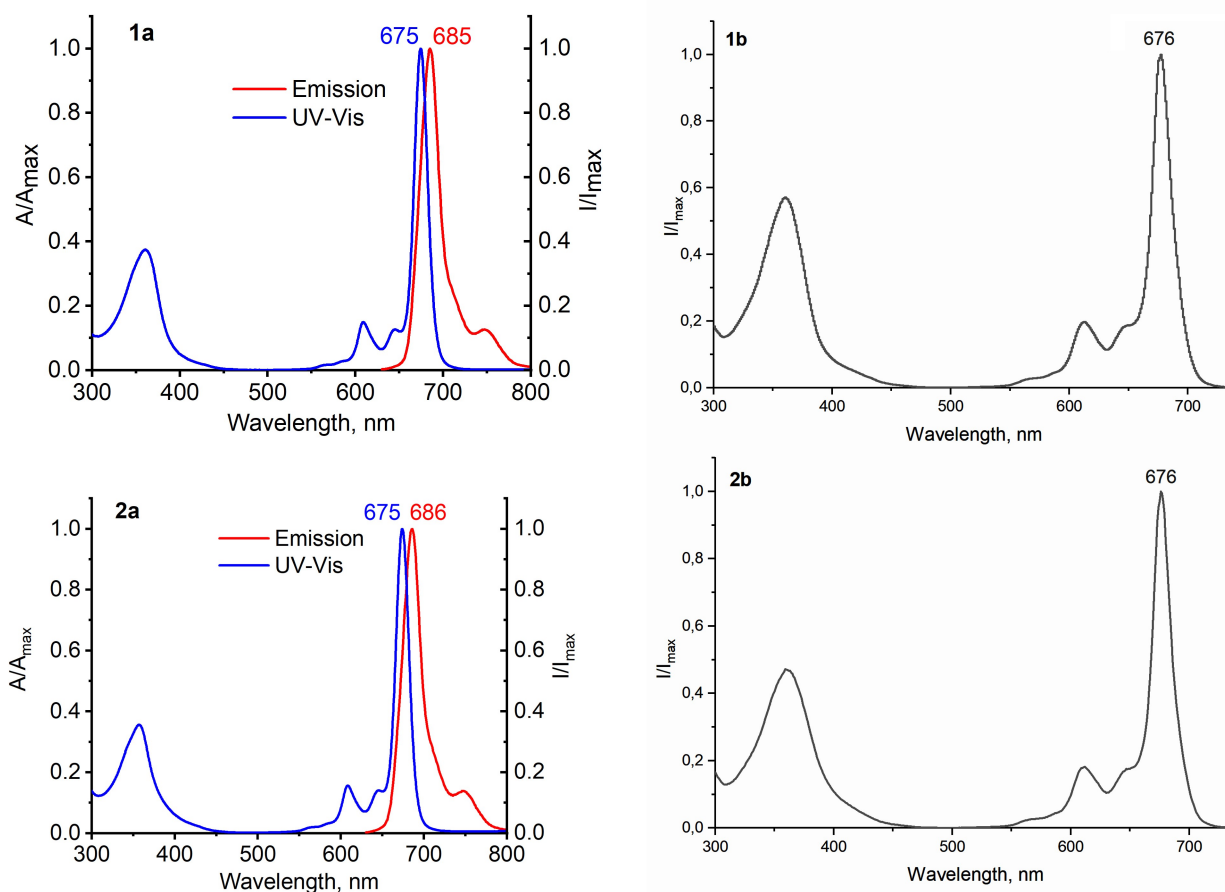


**Figure 6.** **1a, 2a:** Absorption (blue line) and emission (red line,  $\lambda_{ex} = 650$  nm) spectra; **1b, 2b:** luminescence excitation (grey line,  $\lambda_{em} = 687$  nm) spectra of complexes **2** (top) and **3** (bottom) in THF.

The presence of a phenoxy functional group does not affect the quantum yield values (Table 2). At the same time, the nature of the central ion plays a significant role. In the presence of magnesium, the lifetime of the singlet excited state is increased, which leads to an increase in the quantum yield for magnesium phthalocyanines. Unlike unsubstituted phthalocyanines, these complexes dissolve

much better in organic solvents, making them more versatile in their applications.

The results of a thermogravimetric study of the magnesium and zinc complexes indicate their reasonable stability up to 400 °C (Figure 7). In addition to thermogravimetric study the evolved gas analysis was carried out by mass spectrometry. Mass changes at 350 °C can be

attributed to the loss of water (both physically adsorbed and coordinated with  $m/z = 17$  and  $18$ ) as well as other residual solvents. Subsequent temperature increases initiate a number of overlapping processes, leading to the complete destruction of the compound. Oxidation of the complex occurs gradually up to  $800\text{ }^{\circ}\text{C}$  ( $\text{CO}_2$  with  $m/z = 44$ ,  $\text{CO}$  with  $m/z = 28$ , and  $\text{H}_2\text{O}$  with  $m/z = 18$ ).

At  $500\text{--}600\text{ }^{\circ}\text{C}$ , cleavage of fragments of peripheral substituents was observed, in particular, benzene with  $m/z = 78$ ,  $\text{C}_6\text{H}_5\text{O}$  and  $\text{C}_6\text{H}_4\text{O}$  with  $m/z = 93$  and  $94$  respectively,  $p\text{-ClC}_6\text{H}_4\text{O}$  with  $m/z = 127$  and  $128$ . Cleavage of chlorine with  $m/z = 35$  and  $37$  was observed at  $500\text{--}700\text{ }^{\circ}\text{C}$ .

The last step ( $700\text{--}800\text{ }^{\circ}\text{C}$ ) corresponds to the macrocycle of phthalocyanine destruction with its oxidation ( $m/z = 44\text{ CO}_2$ ,  $m/z = 46\text{ NO}_2$ ).

## Conclusions

Octa(*p*-chlorophenoxy) substituted complexes of magnesium and zinc were obtained starting from corresponding phthalonitrile. The target phthalocyanine complexes showed strong absorption at the boundary of the visible and near-IR region with  $\lg\epsilon$  values of about 5. The fluorescence of these complexes was also observed in the range of  $677\text{--}687\text{ nm}$ . The studied complexes demonstrate high values of the fluorescence quantum yield, which doubles when moving from zinc (0.21) to magnesium (0.42) as the central ion. Based on thermal analysis data, these complexes were found to be thermally stable up to  $400\text{ }^{\circ}\text{C}$ .

**Acknowledgements.** Synthesis and identification of target compounds was supported by the Russian Science Foundation Grant No. 24-73-00062. SVE acknowledges (partial) support from M.V. Lomonosov Moscow State University Program of Development.

## References

- Moiseeva E.O., Gorbunova E.A., Dubinina T.V. *Biochemistry (Moscow), Supplement Series B: Biomedical Chemistry* **2024**, *18*, 15–45.
- Vyalkin D.A., Zhabanov Y.A., Tikhomirova T.V., Kazaryan K.Y. *ChemChemTech [Izv.Vyssh. Uchebn. Zaved. Khim. Khim. Tekhnol.]* **2024**, *67* (3), 27–34, doi: 10.6060/ivkkt.20246703.6860.
- Oluwole D.O., Yagodin A.V., Britton J., Martynov A.G., Gorbunova Y.G., Tsvadze A.Y., Nyokong T. *Dalton Trans.* **2017**, *46*, 16190–16198.
- Savelyev M.S., Gerasimenko A.Y., Podgaetskii V.M., Tereshchenko S.A., Selishchev S.V., Tolbin A.Y. *Opt. Laser Technol.* **2019**, *117*, 272–279.
- Klyamer D., Sukhikh A., Nikolaeva N., Morozova N., Basova T. *Sensors* **2020**, *20*, 1893.
- Chindeka F., Mashazi P., Britton J., Oluwole D.O., Mapukata S., Nyokong T. *J. Photochem. Photobiol. A* **2020**, *399*, 112612.
- Koifman O.I., Ageeva T.A., Beletskaya I.P., *et al.* *Macroheterocycles*, **2020**, *13*, 311–467.
- de la Torre G., Claessens C.G., Torres T. *Chem. Commun.* **2007**, 2000–2015.
- Koifman O., Ageeva T., Kuzmina N., *et al.* *Macroheterocycles* **2022**, *15*, 207–302.

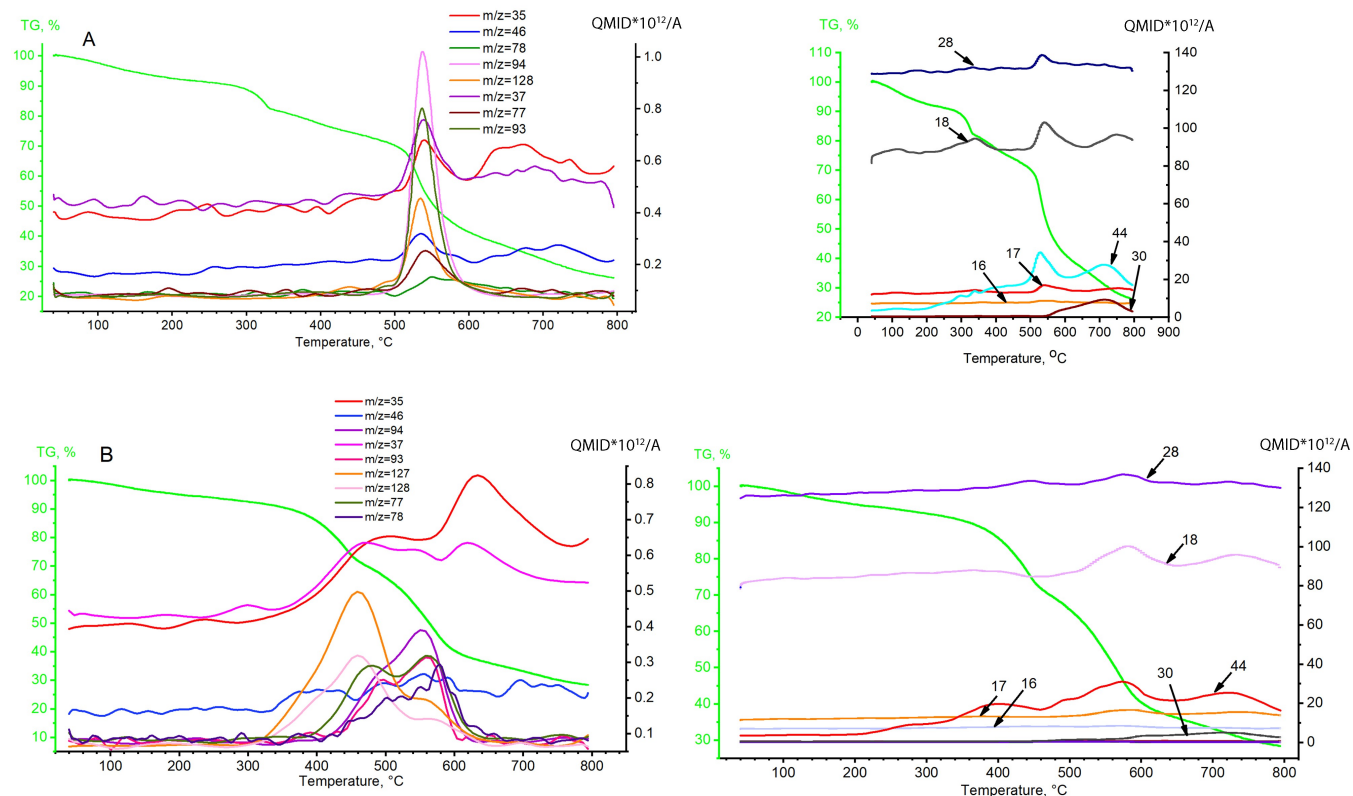


**Figure 7.** Thermogravimetric curves and results of evolved gas analysis by mass-spectrometry for octa(*para*-chlorophenoxy)substituted magnesium (A, top) and zinc (B, bottom) complexes.

11. Xiao Q., Wu J., Pang X., Jiang Y., Wang P., Leung A.W., Gao L., Jiang Sh., Xu Ch. *Curr. Med. Chem.* **2018**, *25*, 839–860.
12. Şenocak A., Köksoy B., Demirbaş E., Durmuş M. *J. Phys. Org. Chem.* **2019**, *32*, e3907.
13. Furuyama T., Miyaji Y., Maeda K., Maeda H., Segi M. *Chem. Eur. J.* **2019**, *25*, 1678–1682.
14. Kuzmina E.A., Dubinina T.V., Borisova N.E., Tomilova L.G. *Macroheterocycles* **2017**, *10*, 520–525.
15. Khabibullin V.R., Gorbunova E.A., Dubinina T.V., Proskurnin M.A. *Macroheterocycles* **2024**, *17*, 205–212.
16. Kavetsou E., Tsoukalas-Koulas C., Katopodi A., Kalospyros A., Alexandratou E., Detsi A. *Bioengineering* **2023**, *10*, 244.
17. Znoyko S.A., Maizlish V.E., Koifman O.I. *ChemChemTech [Izv.Vyssh. Uchebn. Zaved. Khim. Khim. Tekhnol.]* **2024**, *67* (1), 6–35, doi: 10.6060/ivkkt.20246701.6859.
18. Ogunsipe A., Maree D., Nyokong T. *J. Mol. Struct.* **2003**, *650*, 131–140.
19. Brouwer A.M. *Pure Appl. Chem.* **2011**, *83*, 2213–2228.
20. Kousar N., Gorbunova E.A., Dubinina T.V., Sannegowda L.K. *ACS Appl. Energ. Mater.* **2024**, *7*, 7545–7559.
21. Kuzmina E.A., Dubinina T.V., Dzuban A.V., Krasovskii V.I., Maloshitskaya O.A., Tomilova L.G. *Polyhedron* **2018**, *156*, 14–18.
22. Youssef T.E., Ghaffar A.M.A. *J. Appl. Polym. Sci.* **2011**, *119*, 134–141.
23. Znoiko S.A., Petlina A.I., Shaposhnikov G.P., Smirnov N.N. *Russ. J. Gen. Chem.* **2018**, *88*, 1148–1153.
24. Maree S.E., Nyokong T. *J. Porphyrins Phthalocyanines* **2001**, *5*, 782–792.
25. Kuzmina E.A., Dubinina T.V., Zasedatelev A.V., Baranikov A.V., Makedonskaya M.I., Egorova T.B., Tomilova L.G. *Polyhedron* **2017**, *135*, 41–48.
26. Taştemel A., Karaca B.Y., Durmuş M., Bulut M. *J. Luminesc.* **2015**, *168*, 163–171.

Received 05.04.2025

Accepted 30.04.2025